



Title	Measurement of Inherent Deformations in Typical Weld Joints Using Inverse Analysis (Part 1) : Inherent Deformation of Bead on Welding(Mechanics, Strength & Structural Design)
Author(s)	Liang, Wei; Sone, Shinji; Tejima, Motohiko et al.
Citation	Transactions of JWRI. 2004, 33(1), p. 45-51
Version Type	VoR
URL	https://doi.org/10.18910/4410
rights	
Note	

The University of Osaka Institutional Knowledge Archive : OUKA

<https://ir.library.osaka-u.ac.jp/>

The University of Osaka

Measurement of Inherent Deformations in Typical Weld Joints Using Inverse Analysis (Part 1)

Inherent Deformation of Bead on Welding[†]

LIANG Wei*, SONE Shinji*, TEJIMA Motohiko*, SERIZAWA Hisashi **

And MURAKAWA Hidekazu***

Abstract

During welding, deformation occurs as an unavoidable consequence. The Inherent deformation method, in which inherent deformation is introduced into the elastic FEM as the initial strain is one of the effective methods to predict the welding deformation of large structures. When the weld length is long enough, inherent deformation is mainly governed by the heat input Q , and the thickness of plate, h . However, in the assembling of thin plates, a short weld length, between 20-200mm is also often used, especially for thin structures, to reduce distortion. In this case, inherent deformation is influenced not only by the heat input but also by the length of weld. In this research, an efficient measuring method to estimate inherent deformation of plate under bead welding using inverse analysis is developed. Based on this inverse analysis, the inherent deformation is estimated by measuring the three-dimensional coordinates at a small number of selected points. Further, using the estimated inherent deformation, the welding deformation of a plate is predicted as the forward analysis. The distribution characteristic of inherent deformation in short welds is also discussed in this paper.

KEY WORDS: (Inherent deformation), (Inverse analysis), (Welding distortion), (Prediction), (Database).

1. Introduction

Welding is a key technology for building metal structures such as ships, bridges and automobiles. However, it is impossible to avoid welding distortion due to the intrinsic nature of non-uniform heating and cooling of the weldment. Welding deformation not only degrades the performance but also increases the building cost of the structure. In the welding assembly process, welding deformation is also an obstacle for realizing automatization and robotization. In order to solve these problems, it is necessary to quantitatively predict and control welding deformations.

Generally, welding deformations are classified as shown in Fig.1: Longitudinal shrinkage, Transverse shrinkage, Longitudinal bending, Angular distortion, Rotational distortion, Buckling distortion. In principle, there are three fundamental types of deformation, namely the longitudinal shrinkage, the transverse shrinkage and the angular distortion that occur during the

welding process and cause various forms of distortion in welded structures. These three types of deformation can be regarded as fundamental inherent deformations due to welding.

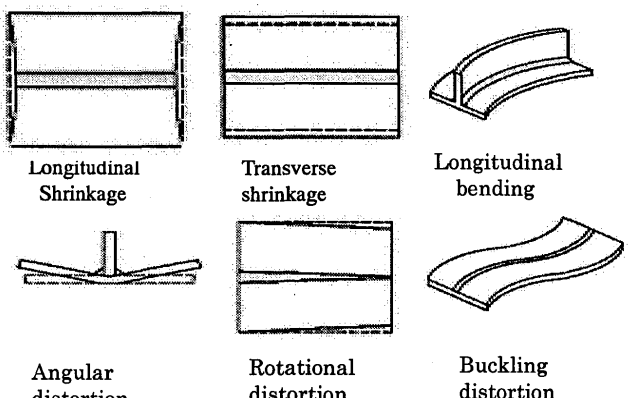


Fig. 1 types of welding deformation

When the welding line is long enough, the distribution

† Received on June 8, 2004

* Graduate student

**Associate Professor

*** Professor

Transactions of JWRI is published by Joining and Welding Research Institute of Osaka University, Ibaraki, Osaka 567-0047, Japan

of the inherent deformation along the welding line can be assumed to be a constant value, which is mainly determined by the heat input Q , the thickness of the plate, h , and the type of joint¹⁾. As an example, the relationship between angular distortion under the bead on plate welding and the heat input parameter Q/h^2 is illustrated in Fig.2. As seen from the figure, the inherent deformation can be regarded as a function of the heat input parameter Q/h^2 . Once the inherent deformations are given as functions of the heat input parameter, welding deformation of large welded structures like the structure shown in Fig.3 can be predicted by an elastic finite element method using the concept of inherent deformation²⁾.

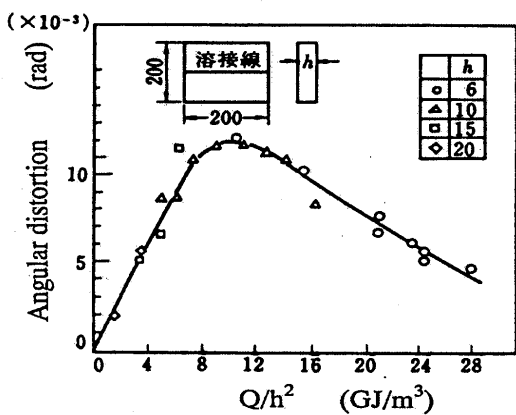


Fig. 2 Relationship between angular distortion And Q/h^2

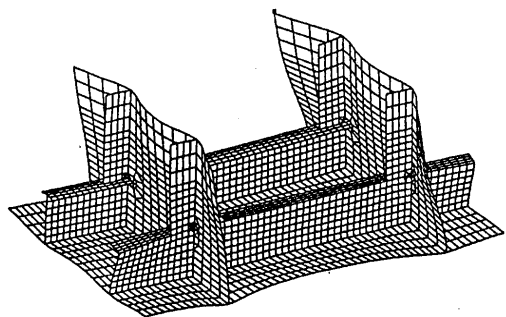


Fig. 3 Welding distortion of ship structure calculated by elastic FEM analysis

However, in the welding assembly of thin plates, a short weld length between 20~200mm is frequently employed. In this situation, the inherent deformation is affected not only by the heat input, Q , and the thickness of the plate, h , but also by the length of the weld, because the welding line is shorter than the length of the welded part.

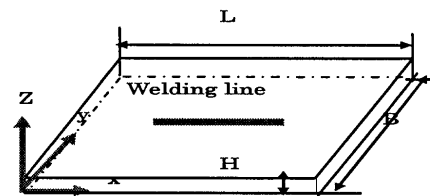
In this work, at first, we studied the distribution characteristic of the inherent deformation along the welding line for a weld with short length. Then a simple

measuring method of welding inherent deformation using inverse analysis was proposed. Based on the inverse analysis, the inherent deformation was estimated by measuring the three-dimensional coordinates at a small number of selected points. Finally, using the determined inherent deformations, the welding deformation was predicted as a forward analysis.

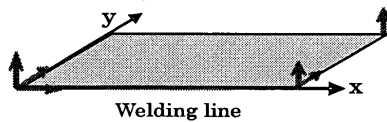
2. Distribution characteristic of inherent deformation

When the welding line is shorter than the length of the plate to be welded, the weld length has a large influence on the inherent deformation. Therefore, we studied the distribution characteristic of inherent deformation along welding line at first.

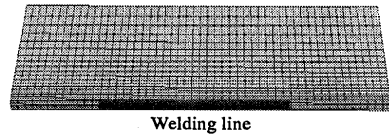
Generally, for the weldment with long weld lengths, two methods can be used to obtain the inherent deformation. One is the experimental method and the other is the numerical simulation using the thermal-elastic-plastic finite element method. In order to obtain the detailed information of inherent deformation and to clarify its distribution characteristic along the welding line for a short weld, a thermal-elastic-plastic finite element method was employed in this study.



(a) the dimension of the model



(b) boundary condition



(c) mesh division

Fig.4 FEM model and boundary condition

The procedure to compute the inherent deformation using the thermal-elastic-plastic three-dimensional finite element method is presented in this section. The partial bead welding on a flat plate as shown in Fig.4 (a) is

taken as an example. Half of the model is analyzed due to the symmetry. The dimensions, the boundary condition and the mesh division are shown in Fig.4.

The dimensions of the model are: $L=200$ mm, $B=100$ mm and $h=2.5$ mm. The weld heat input and the welding speed were assumed as 160 J/mm and 15 mm/sec. The middle part of the plate is assumed to be welded. The length of the weld is 100 mm in this case.

The half plate is uniformly divided into 50 and 4 elements in the welding and the thickness directions. The FEM model had 4000 brick elements and 5355 nodes. It had a fine grid in the welding zone.

To clarify the distribution characteristic of the inherent deformation along welding line and the influence of the initial temperature, four cases are analyzed. The initial temperature of cases A, B, C, D were assumed as 20 °C, 100 °C, 200 °C and 300 °C, respectively.

The material of the plate is SUS304, the temperature dependent thermal and mechanical properties are used in the analysis. The problem is solved using ABAQUS employing the "DC3D8" element and "C3D8I" element for thermal and stress analysis, respectively.

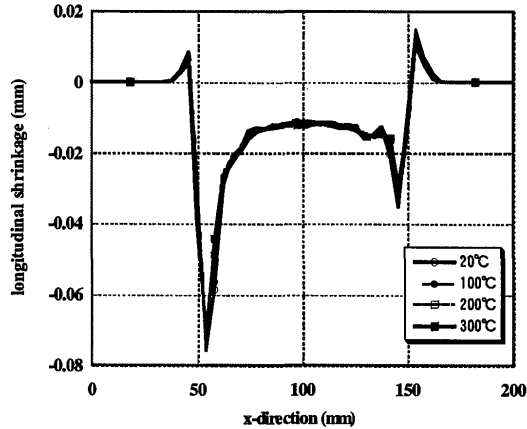


Fig. 5 Distribution of longitudinal shrinkage along welding line.

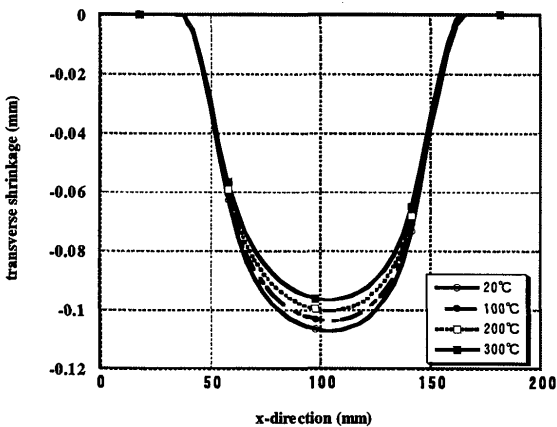


Fig. 6 Distribution of transverse shrinkage along welding line.

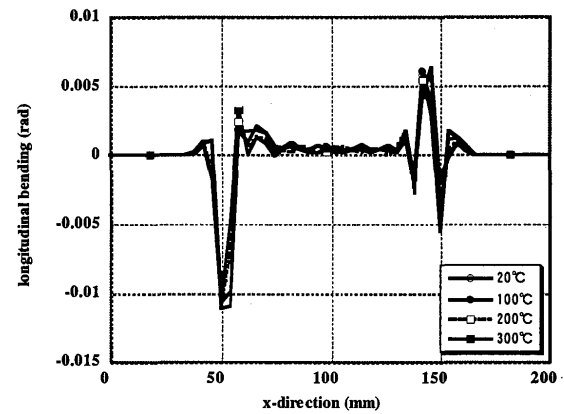


Fig. 7 Distribution of longitudinal bending along welding line.

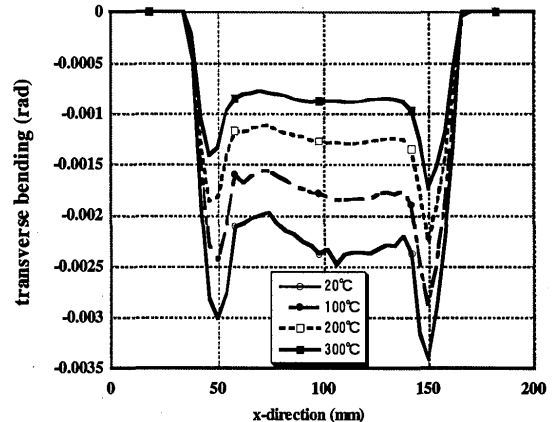


Fig. 8 Distribution of transverse bending along welding line.

The welding distortion is assumed to be caused by four components, namely longitudinal shrinkage δ_x^i , transverse shrinkage δ_y^i , longitudinal curvature θ_x^i and transverse curvature θ_y^i . These four components of inherent deformation can be defined by the following equations:

$$\begin{aligned}\delta_x^i &= \int \varepsilon_x^i dy dz / h \\ \delta_y^i &= \int \varepsilon_y^i dy dz / h \\ \theta_x^i &= \int \varepsilon_x^i (z - h/2) / (h^3/12) dy dz \\ \theta_y^i &= \int \varepsilon_y^i (z - h/2) / (h^3/12) dy dz\end{aligned}\quad (1)$$

Where, ε_x^i is the plastic strain in the welding direction x, and ε_y^i is that in the y direction. The values of ε_x^i and ε_y^i can be obtained as the results of the thermal-elastic-plastic FEM analysis.

The distributions of the inherent deformation are shown in Figs. 5 ~8. From these figures, it is seen that:

- (1) Although inherent deformation varies along the welding line, the variation is not large in the middle part of the welding.
- (2) Due to the end effect, the variation of inherent

deformation is very large at both ends of the welding line.

(3) The initial temperature has a small influence on the distributions of longitudinal shrinkage and bending. On the other hand, a significant influence is observed in transverse shrinkage and bending. With the increase of initial temperature, the maximum values of transverse shrinkage and bending reduce.

3. Method of analysis

3.1 The elastic analysis of welding deformation using inherent strain method

Using the welding inherent deformation obtained through the procedure presented in the preceding section, the average values of the inherent deformation can be calculated. The average value of the inherent deformation is defined as the integration of the inherent deformation divided by the weld length. Using the average value of the inherent deformation, the welding deformation is predicted by an elastic FEM. As one of the results, the distribution of displacement in the z direction (deflection) is shown in Fig.9. Meanwhile, the result obtained by thermal-elastic-plastic FEM analysis is shown in Fig.10. As seen from the two figures, the deflection predicted by the elastic FEM agrees fairly well with that by the thermal-elastic-plastic FEM.

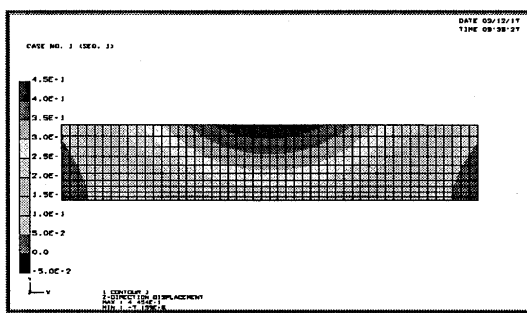


Fig. 9 Welding distortion calculated by elastic FEM analysis.

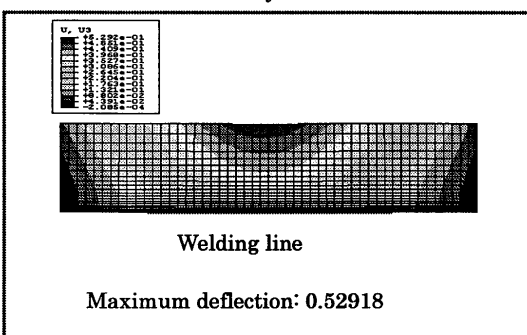


Fig. 10 Welding distortion calculated by elastic-plastic FEM.

Thus, the average value of the inherent deformation can be used as an approximation to predict the welding deformation of plate with short welds.

3.2 Measurement of Welding Inherent Deformation by Inverse analysis

If the distribution of the welding inherent deformation is expressed in terms of a small number of parameters, the inherent deformation can be determined through inverse analysis based on the measurement of the deformation at limited locations. In this study, a method of inverse analysis is proposed under the following hypotheses:

- (1) The four components, namely longitudinal shrinkage, transverse shrinkage, longitudinal curvature and transverse curvature are regarded as the components of inherent deformations to be determined.
- (2) If the distribution function of each component of the inherent deformation is expressed by n parameters, the total number of parameters is $4n$.
- (3) The length and the width of the area where the inherent deformation is distributing can be determined by the thermal-elastic-plastic FEM analysis.
- (4) The three-dimensional coordinates of m points are measured before and after the welding.

Since the coordinates measured at m points include the rigid body motion, the number of linearly independent relationships is $(3m-6)$. Thus, the necessary condition for determining the inherent deformation is: $(3m-6) > 4n$.

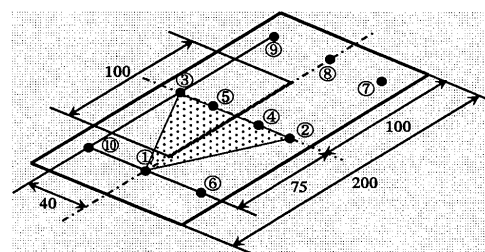


Fig. 11 Measurement points for inverse analysis.

Based on the above idea, the ten points on the specimen as shown in Fig.11 were selected. By measuring the three-dimensional coordinates of the 10 points, the inherent deformation can be determined according to the following procedure:

- (1) In order to exclude rigid body motion, the base triangle is defined. The base triangle consists of points 1, 2, 3 as shown in Fig.11.
- (2) From the coordinates of three vertexes belonging to the base triangle, the stretch of each side gives three independent relations.

(3) Concerning the other measuring points, except the points forming the basic triangle, the variations of the distances between each point and the 2 points of the basic triangle give $2(m-3)$ conditions, similarly, from the variations of the normal distance between each point and the plane defined by the basic triangle, $(m-3)$ conditions can be obtained.

(4) Adding (2) and (3), the number of the total relations becomes $(3m-6)$.

(5) The relations defined in (2) and (3) are basically the equations relating the inherent deformation a_i and the deformation of the specimen F_j^m , such as the stretch between two points or the deflection relative to the base triangle, i.e.

$$F_j(a_i) = F_j^m \quad (2)$$

where, a_i : components of inherent deformation

$F_j(a_i)$: deformation of specimen which is computed by FEM using inherent deformation a_i

F_j^m : measured deformation

(6) Since the relation between the inherent deformation a_i and the deformation of the specimen $F_j(a_i)$ is nonlinear, the function $F_j(a_i)$ is nonlinear. Therefore, the inherent deformation a_i can not be determined from the measured value F_j^m by a single step. It must be determined through an iterative process based on the following Taylor expansion.

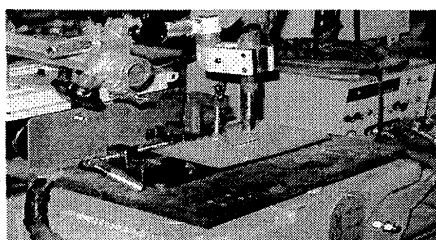
$$F_j(a_i + \Delta a_i) \approx F_j(a_i) + (\partial F_j / \partial a_i) \Delta a_i = F_j^m \quad (3)$$

or in matrix form,

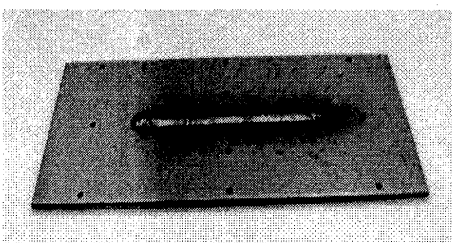
$$\left[\frac{\partial F_j}{\partial a_i} \right] \{ \Delta a_i \} = \{ F_j^m - F_j(a_i) \} \quad (4)$$

where, Δa_i is the correction to the approximate solution at the previous step.

4. Example of application



(a) welding apparatus



(b) test specimen

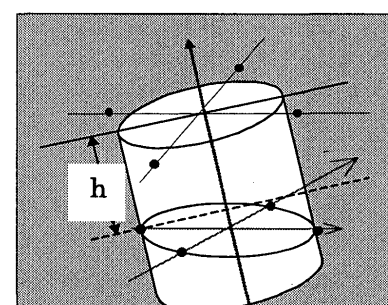
Fig. 12 Welding experiment

In order to examine the effectiveness of the proposed inverse analysis to estimate the inherent deformation, bead welding on a flat steel plate is chosen as an example. A photo of the welding apparatus and the test specimen is shown in Fig. 12. As seen from Fig. 12(b), circular holes are made at ten points where the three-dimensional coordinates before and after the welding are measured.

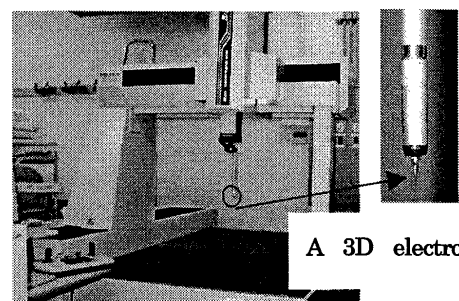
The length, the width and the thickness of the model are 200 mm, 100 mm, and 3 mm, respectively. The bead weld is made by MAG welding. The length of the weld is 100 mm. The welding current, the arc voltage and the welding speed are 100 A, 20V, and 20 mm/s, respectively.

4.1 Measurement of welding deformation

In order to measure the welding deformation at the center of the circular hole, three-dimensional coordinates at 8 points around the hole shown in Fig.13 (a) are measured. Of these, 4 points are located on the top surface of the plate and they are used to find the surface of the plate. The coordinates of the remaining 4 points in the hole are used to locate the axis of the cylindrical hole. The 3D-coordinates of each point are measured by the 3D measurement system shown in Fig.13 (b). When the probe touches the specimen, the 3D-coordinates are recorded. Using the coordinates of 8 points, the coordinates at the center of the hole are calculated.



(a) measurement points



(b) 3D-measurement system

Fig. 13 measurement of welding deformation

4.2 Computed results and discussion

Using the coordinates of the ten points measured before and after welding, the four components of the inherent deformation are estimated by the inverse analysis described above. To examine the validity of the estimated inherent deformations, the welding deformation produced by these inherent deformations is computed as a forward analysis and compared with the measured values.

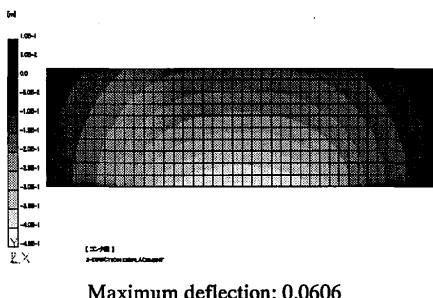


Fig. 16 Predicted deflection of specimen.

Table 1 Comparison of welding distortion between measurements and computations.

relative deflection	Dire- ction	Measure ment (mm)	Forward Analysis (mm)
$W_3 \cdot (w_9+w_{10})/2$	z	0.1044	0.1066
$W_8 \cdot (w_7+w_9)/2$	z	0.0783	0.0742
$W_1 \cdot (w_{10}+w_6)/2$	z	0.0707	0.0714
$(W_2+W_3)/2$ $-(w_4+w_5)/2$	z	0.1400	0.1400

As an example of computed results, the distribution of the displacement in the z direction (deflection) is shown in Fig.14, the relative deflection obtained by the measurement and those obtained by the forward FEM analysis are shown in Table 1. As seen from the table, the two results show good agreement. This proves the accuracy of the 4 components of the inherent deformation determined by using the proposed inverse analysis.

4.3 Influence of welding length:

As demonstrated above, the proposed method is effective for determining the 4 components of the inherent deformation. Thus, it can be employed to build up a database of the inherent deformation. Once the database is established, the welding deformation of large welded structure can be predicted by using elastic FEM.

In this research, a database of inherent deformation

has been built up according to Table 2. As an example, the relations between transverse shrinkage and heat input parameter Q/h^2 are shown in Fig.15 for the welding with lengths of 20 mm, 50 mm, 100 mm, 130mm, respectively. As seen from the figure, the transverse shrinkage is significantly small when the weld length is small, such as the case of 20mm. The transverse shrinkages are almost the same when the weld length is greater than 50mm.

Table 2 Range of parameters covered by database.

Typical Weld joint		Butt joint Fillet joint Lap joint
Weld length		20 mm 50 mm 100 mm 130 mm
Welding parameter	Welding current	100 A 200 A
	Arc voltage	18-20V
	Welding speed	10 mm/s 15 mm/s 20 mm/s
The thickness of plate		2 mm 3 mm

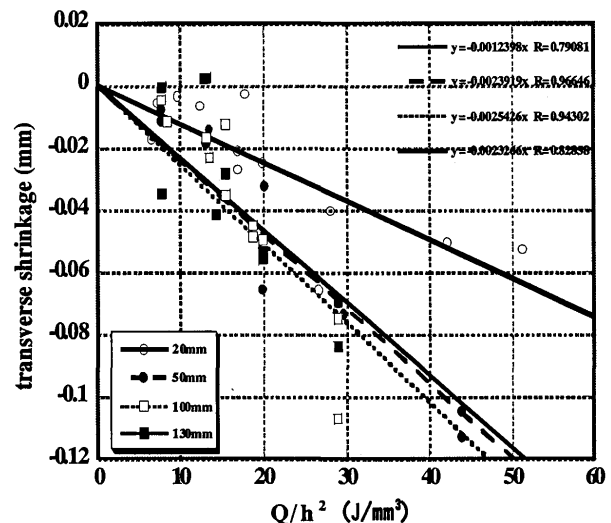


Fig. 15 Relations between transverse shrinkage and heat input parameter Q/h^2 .

5. Conclusions

The distribution of the inherent deformation for partial bead on plate welding is clarified using thermal-elastic-plastic FEM analysis. Based on this knowledge, a simple method to estimate the inherent

deformation by inverse analysis is proposed. Through the present work the following conclusions are drawn.

(1) The values of the inherent deformations vary along the welding line in partial welding just as in the case of full welding. The variation is small in the middle part, but at both ends is very large.

(2) The preheating temperature affects the transverse shrinkage and the bending. Its effect on the longitudinal shrinkage and the bending is small.

(3) The distribution of inherent deformation can be approximated by uniformly distributed shrinkage and bending in the longitudinal and transverse directions.

(4) The four components of the inherent deformation under bead welding can be estimated using the proposed inverse analysis.

(5) It is shown that the welding deformation under partial bead on plate welding can be reproduced by elastic FEM using the estimated inherent deformation with sufficient accuracy.

(6) Significant influence of the weld length to transverse shrinkage is observed when the weld length is short, such as the case of 20mm.

References

- 1) Kunihiko Satoh and Toshio Terasaki. "Effect of welding condition on welding Deformation in welded structural Materials", Journal of the Japan Welding Society, Vol.45, pp.302-308, (1976).
- 2) Dean Deng, Hidekazu Murakawa and YuKio Ueda. "Theoretical prediction of welding distortion considering positioning and Gap Between Parts", International Journal of offshore and polar Engineering, (2004).
- 3) Yu Luo, Hidekazu Murakawa, Morinobu Ishiyama . "Study on Welding Deformation of Plate with Longitudinal Curvature", Symposium of Welding structure, pp.311-317, (1999).